



## Hypogene Evaporite Karst Geohazards: Implications for Energy Sector Infrastructure in the Delaware Basin, USA

K. W. Stafford, W. A. Brown, and L. D. Perkins

Department of Geology, Stephen F. Austin State University, Nacogdoches, Texas 75962

### ABSTRACT

Hypogene karst is well recognized throughout the greater Permian Basin of Texas and New Mexico (USA) and has traditionally presented geohazard risks to drilling operations. Recent advances in petroleum engineering have enabled new exploitation of resources within the Delaware Basin interior, including the Gypsum Plain, which hosts abundant karst geohazards, both epigene and hypogene. Rapid oil field growth has expanded infrastructure development within the Gypsum Plain and heavily affected existing roadways not originally designed for energy sector activity. Infrastructure is commonly affected by shallow geohazards with greatest risk intensity in areas affected by hypogene processes. Geohazards manifest to variable degrees as road subsidence and collapse, often due to road base failure that are amplified by anthropogenic modification of the natural geomorphology. Caves, intrastratal dissolution, brecciation, diagenetic alteration (e.g., evaporite calcitization), and intermittent artesian conditions create unique variants of hypogene geohazards.

Current research on Gypsum Plain geohazards utilizes a multidisciplinary approach that couples traditional field surveys with geographic information system and geophysical remote sensing analyses. Electrical resistivity tomography has been successfully implemented as an efficient and effective method for characterization of potential karst geohazards, specifically delineation of the extent and occurrence of hypogene geohazard phenomena that are not well expressed at the land surface. Capacitively Coupled (CC) resistivity techniques enable rapid collection of shallow geophysical data, while Direct Current (DC) resistivity techniques produce more detailed subsurface imaging to greater depths. The coupling of these techniques provides accurate subsurface delineation of potential hypogene geohazards to facilitate development of improved infrastructure design by civil engineers in order to mitigate geohazard risk.

## INTRODUCTION

The Permian Basin of Texas and New Mexico has been a major petroleum-producing province for the past century and recent advances in petro-engineering techniques have enabled exploitation of unconventional resources in the Wolfcamp Shale and Bone Springs Formation within the Delaware Basin interior. These unconventional reservoirs alone contain an estimated 6.3 billion metric tonnes (46.3 billion barrels) of oil and 7.96 trillion cubic meters (281 trillion cubic feet) of associated gas (USGS, 2018), thus resource exploitation has significantly increased oilfield activity within the Delaware Basin where evaporite karst is extensive. While known hypogene karst is widespread throughout Permian Basin carbonates (e.g., Kirkland, 2014), research over the last decade has also documented abundant hypogene karst in evaporite strata (e.g., Stafford et al., 2018).

Various techniques have been developed to characterize Gypsum Plain karst phenomena. Currently, coupling of GIS (Geographic Information System) techniques with geophysical methods is proving to be the most effective method for delineation of karst features and more importantly potential karst geohazards. However, traditional field mapping and a priori knowledge of lithology and diagenetic alternations associated with karst processes in the region is essential for accurate geohazard assessment. Stafford et al. (2008) produced the first spatial distribution map of Gypsum Plain karst through orthoimagery analyses. Ehrhart (2016) demonstrated the effectiveness of high-resolution digital elevation models derived from LiDAR (Light Detection and Ranging) analyses for improved spatial delineation of subtle surficial manifestations of karst. Majzoub et al. (2017) were the first to demonstrate effectiveness of electrical resistivity for detection and characterization of shallow evaporite karst geohazards within the Gypsum Plain in Texas while Land et al. (2018) further demonstrated this effectiveness in New Mexico. Majzoub et al. (2017) and Land et al. (2018) both utilized DC (Direct Current) electrical resistivity tomography, while Stafford et al. (2017) and Woodard (2017) demonstrated that CC (Capacitively Coupled) electrical resistivity techniques provide an equally effective method for shallow karst geohazard detection.

## METHODS

Evaporite geohazard research by the authors utilizes both CC and DC resistivity techniques as each has advantages and disadvantages. CC resistivity methods enable continuous data collection at rates up to ~3.5 km/hr, but depth of data resolution is rarely more than 5 m. DC resistivity methods enable greater depth of resolution, generally 20–80 m depending on electrode spacing; however, DC resistivity surveys are time intensive (a single 112-electrode-survey averages more than four hours).

CC resistivity imaging was collected continuously along >100 km of asphalt-paved and unimproved roadway in Culberson County, Texas, using a Geometrics TR5 OhmMapper in a dipole-dipole array composed of five receivers connected by 2.5 m coaxial cables with a transmitter offset of 2.5 m. Data was collected at a transmission rate of once per second and traverse speed of ~1 m/sec. GPS (Global Positioning System) data for positioning was collected simultaneously with a Trimble Nomad 900 series logger connected to a Zephyr antenna having a horizontal accuracy of <50 cm.

DC resistivity imaging was collected at more than thirty isolated sites where greater depth of resolution was warranted using an AGI (Advanced Geoscience Inc.) SuperSting R8/IP multi-electrode resistivity meter in a dipole-dipole array. For all DC resistivity surveys, measurement time was set to 1.2 s and cycled twice per electrode pair; maximum error threshold between measurement cycles was set at 2% and current injection set to a maximum of 2000 mA. Prior to each DC resistivity survey, electrode sites were wetted with a dilute saline solution to reduce electrical contact resistance with the ground.

Data acquired through both CC and DC resistivity imaging were processed with AGI's EarthImager 2D software. Resistivity pseudosections were inverted with default settings and

smooth model inversion; a maximum of 5% of modeled misfit data was removed based on inversion histogram analyses. Terrain corrections were applied to resistivity data through extraction of elevation data from digital elevation models having a 10cm vertical accuracy created from bare earth LiDAR data. Four sites from Culberson County, Texas (Fig. 1), are presented as examples of the diversity of hypogene geohazard characterization utilizing electrical resistivity imaging.

## RESULTS

Example 1 (Fig. 2) is a CC electrical resistivity that demonstrates a non-uniformly cemented breccia pipe formed from a combination of upward stoping collapse and evaporite calcitization through hypogene processes. The land surface exhibits less than 30 cm of vertical variation with proximal surface exposures of indurated gypsic soil, poorly cemented gypsum breccia, and variably cemented calcitized breccia. The resistivity image presented in Figure 2 is centered on the calcitized portion of the breccia pipe that extends from -15 m to -110 m along the resistivity profile. Within the core of the breccia pipe, dense, well-cemented calcitized breccia and porous, poorly cemented, calcitized regions are discernable, which correlate well with proximal surface exposures. Gypsum extends from the edges of the breccia pipe; brecciated gypsum is at the boundary of calcitization and un-brecciated gypsum is distal to the contact.

Example 2 (Fig. 3) is a CC electrical resistivity that demonstrates solution widened fractures produced by ascending fluids. However, associated surficial geomorphic features were destroyed during road construction and -1.5 m of locally-derived fill material was used for road-base leveling. While topographic ridges can be observed in proximal undisturbed landscape, these structures were destroyed during road construction. These hypogene features now manifest in resistivity data as a series of solutionally-widened fractures in gypsum that are partially filled with indurated gypsite which is being actively piped downward from overlying roadbase fill; the upper 1-2 m of the resistivity profile contain roadbase fill with a higher clay content that retains greater moisture. Observations of similar features that have not been impacted by road construction indicate gypsic soils piping into hypogene fractures are being actively modified by condensation corrosion. The gypsum fraction of the soil is being dissolved by high moisture content within the fracture while insoluble residue is continuously piped downward.

Example 3 (Fig. 4) is a DC electrical resistivity that demonstrates intrastratal leaching of bedrock in a topographic low region where multiple, low-volume artesian discharge loci occurred in September 2014. Surface morphology was slightly modified during road construction, including the addition of -60 cm of roadbase composed of locally derived fill materials to raise the road surface and minimize ephemeral ponding on pavement. Electrical resistivity data analyses indicate discontinuous regions of competent gypsum bedrock at depths >5 m that are mixed with low resistivity regions indicative of higher moisture content gypsum bedrock having significant leached porosity induced by artesian leaching. Excavations revealed that gypsum bedrock in these regions are heavily leached and heterogeneous, which results in differential subsidence geohazards.

Example 4 (Fig. 5) is a DC electrical resistivity that demonstrates intrastratal collapse at a roadcut section through Rustler strata. Resistivity data analyses indicate that the subsurface is dominated by moderate resistivity media containing discontinuous high resistivity "lenses" of a secondary geologic medium. Rustler strata has differentially settled and fractured from intrastratal dissolution of underlying Salado evaporites, thus creating highly permeable media that exhibit minor solutional widening along abundant fractured carbonate surfaces and bedding planes. Rustler carbonate is characterized by low to moderate resistivity values; residual Rustler gypsum is discontinuous and represented by high electrical resistivity. Rustler gypsum is porous and recrystallized based on field excavation, and alteration decreases towards the center of residual gypsum masses. Low electrical resistivity regions are interpreted to contain pore fluids with elevated sulfate content from meteoric dissolution and transport of residual Rustler gypsum.

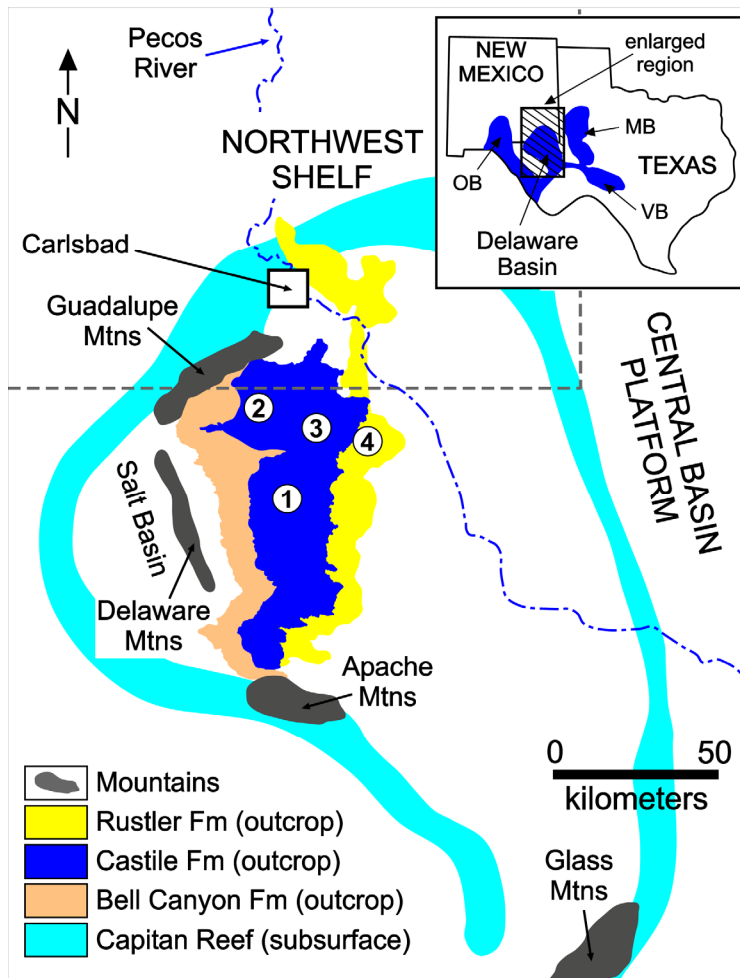


Figure 1. Location of study area, including four example site locations numbered accordingly in white circles, in relation to major geomorphic/geologic structures within the region and outcrop areas of important geologic strata. MB = Midland Basin, VB = Val Verde Basin, and OB = Orogrande Basin.

## SUMMARY AND CONCLUSIONS

Hypogene karst phenomena throughout the Gypsum Plain are diverse, including traditional hypogene phenomena formed in confined conditions (e.g., hypogene caves, breccia pipes) and associated diagenetic alteration (e.g., evaporite calcitization, sulfur ore emplacement). Non-traditional hypogene phenomena related to unconfined conditions (e.g., artesian discharge, condensation corrosion) further complicate speleogenesis by creating unique structures or overprinting existing karst phenomena. Therefore, knowledge of regional karst variability and hydrogeology coupled with field mapping and remote sensing methods are essential for detection, delineation, and characterization of karst geohazards of the Gypsum Plain, especially those formed through hypogene processes that are either minimally expressed or not expressed at the land surface.

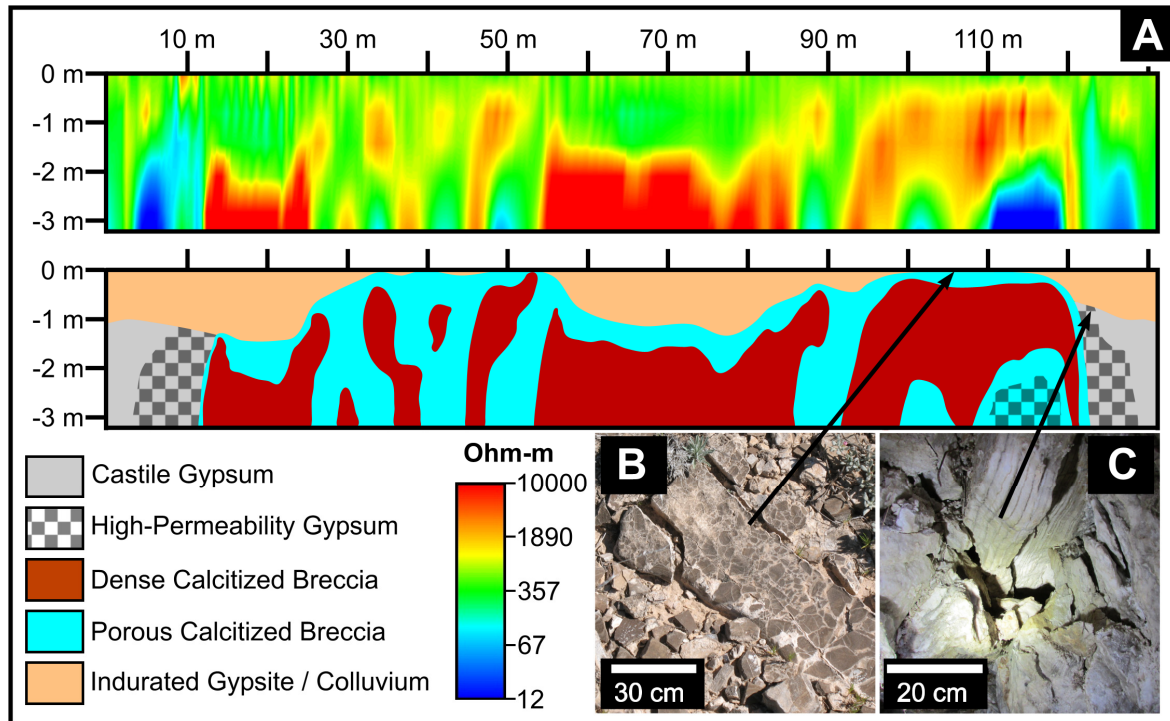


Figure 2. Breccia pipe geohazard (example 1): (A) CC electrical resistivity profile (RMS [Root Mean Square] error = 8.16%) and associated interpretation, including dense and porous calcitized breccia in relation to gypsum and high permeability regions at feature margins; (B) image of typical surficial exposure of calcitized gypsum breccia; and (C) image of typical gypsum breccia at margin of breccia pipe.

Remote sensing techniques are utilized for characterization of karst development throughout the Gypsum Plain. Electrical resistivity techniques have been successfully used to delineate shallow geophysical anomalies, but require a combination field mapping and occasional excavation for proper characterization. CC electrical resistivity tomography has proven to be an efficient method for rapid data collection of shallow karst phenomena while DC electrical resistivity tomography has enabled greater depth and resolution of problematic karst phenomena. Currently, these methods are being utilized to improve road design and efficiently mitigate karst geohazards.

### ACKNOWLEDGMENTS

The authors thank Texas Department of Public Transportation and Stephen F. Austin State University for partial research funding support for this project.

### REFERENCES CITED

Ehrhart, J., 2016, Speleogenesis and delineation of megaporosity and karst geohazards through geologic cave mapping and LiDAR analyses associated with infrastructure in Culberson County, Texas: M.S. Thesis, Stephen F. Austin State University, Nacogdoches, 164 p.

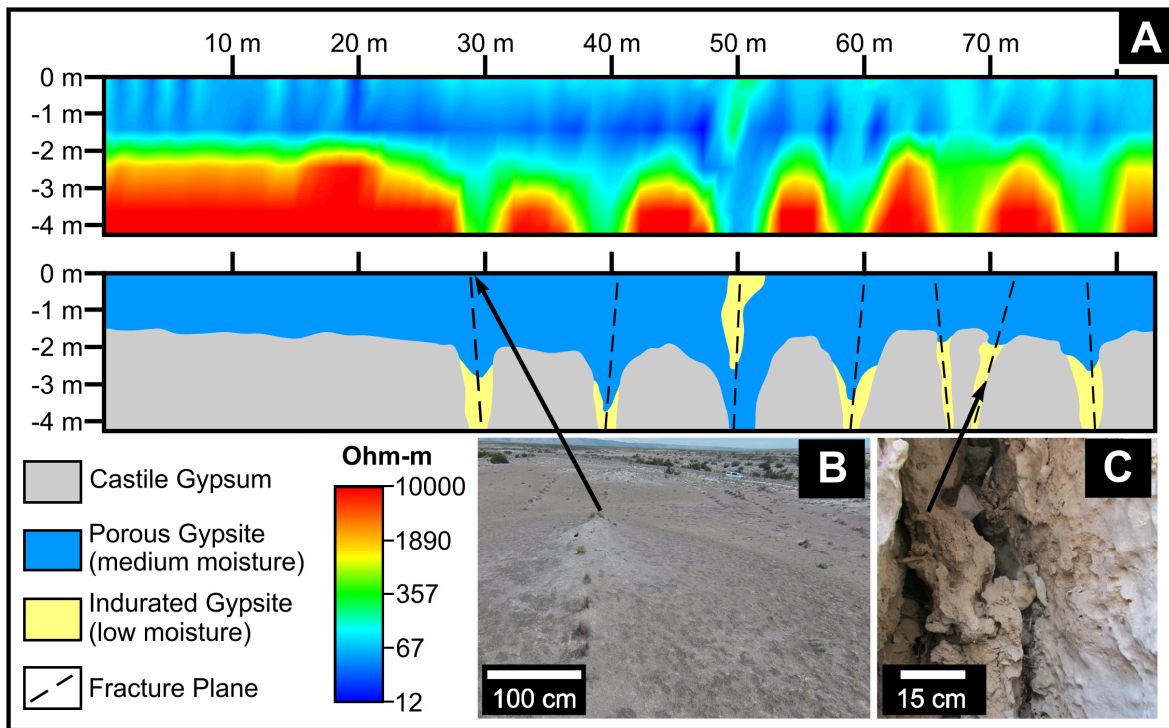


Figure 3. Fracture vent geohazard (example 2): (A) CC electrical resistivity inversion profile (RMS error = 6.00%) and associated interpretation that shows solution-widened fractures, indurated gypsite, and porous gypsite introduced as roadbase fill during constructions; (B) typical unaltered geomorphic surface showing topographic ridges associated with fracture vents that are commonly destroyed during road construction; and (C) example of fracture vent with partial, indurated gypsite fill.

Kirkland, D., 2014, Role of hydrogen sulfide in the formation of cave and karst phenomena in the Guadalupe Mountains and western Delaware Basin, New Mexico and Texas: National Cave and Karst Research Institute, Carlsbad, 77 p.

Land, L, C. Cikoski, D. McCraw, and G. Veni, 2018, Karst geohazards and geophysical surveys: US 285, Eddy County, New Mexico: National Cave and Karst Research Institute Report of Investigation 7, Carlsbad, 89 p.

Majzoub, A., K. Stafford, W. Brown, and J. Ehrhart, 2017, Characterization and delineation of gypsum karst geohazards using 2-D electrical tomography, Culberson County, Texas, USA: *Journal of Environmental and Engineering Geophysics*, v. 22, no. 3, p. 441-420.

Stafford, K., W. Brown, J. Ehrhart, A. Majzoub, and J. Woodard, 2017, Evaporite karst geohazards in the Delaware Basin, Texas: review of traditional karst studies coupled with geophysical and remote sensing characterization: *International Journal of Speleology* v. 46, no. 2, p. 169-180.

Stafford, K., J. Ehrhart, A. Majzoub, J. Shields, and W. Brown, 2018, Unconfined hypogene evaporite karst: West Texas and southeastern New Mexico, USA: *International Journal of Speleology*, v. 47, no. 3, p. 293-305.

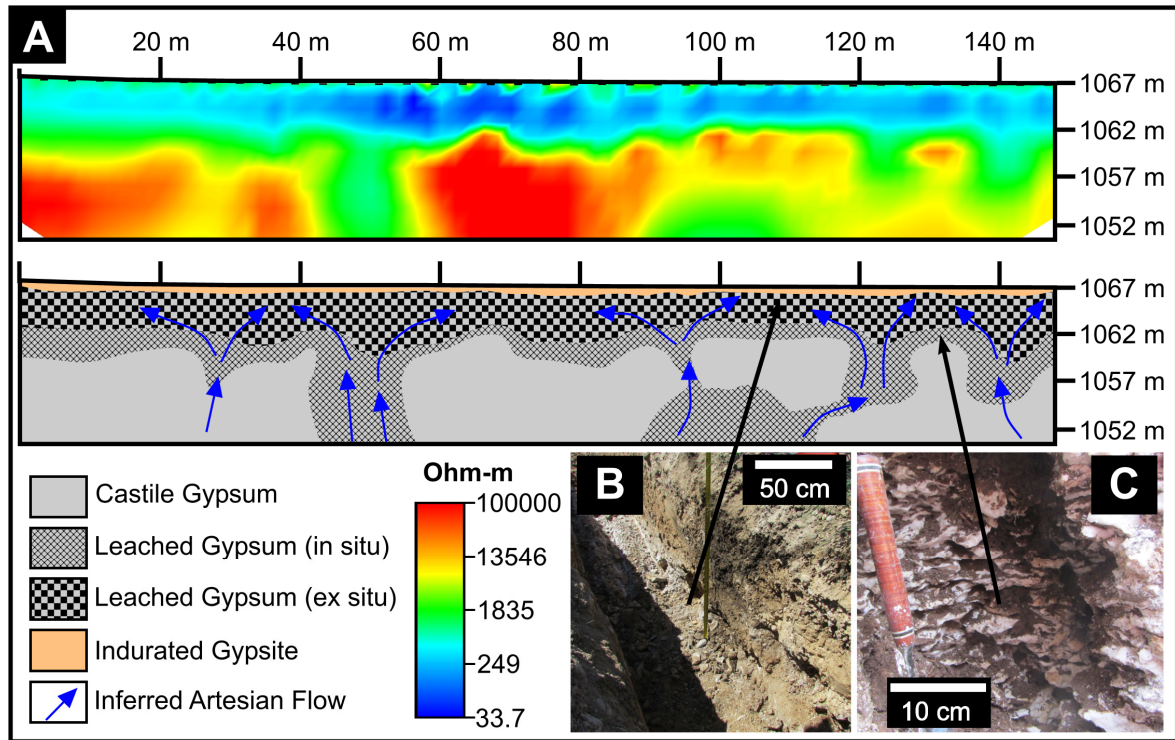


Figure 4. Intrastratal leaching geohazard (example 3): (A) DC electrical resistivity profile (RMS error = 4.44%) and associated interpretation of heavily leached gypsum in region of documented artesian discharge including locally displaced (ex situ) leached bedrock that was buoyantly lifted during artesian discharge; (B) trench excavation showing partial wall collapse near base in ex situ leached gypsum; and (C) trench excavation in competent, in situ leached gypsum.

Stafford, K., L. Rosales-Lagarde, and P. Boston, 2008, Castile evaporite karst potential map of the Gypsum Plain, Eddy County, New Mexico and Culberson County, Texas: A GIS methodological comparison: *Journal of Cave and Karst Studies*, v. 70, no. 1, p. 35-46.

USGS (U.S. Geological Survey), 2018, Assessment of undiscovered continuous oil and gas resources in the Wolfcamp Shale and Bone Spring Formation of the Delaware Basin, Permian Basin Province, New Mexico and Texas, 2018: U.S. Geological Survey Fact Sheet 2018-3073, 4 p.

Woodard, J., 2017, Geophysical delineation of megaporosity and fluid migration pathways for geohazard characterization within the Delaware Basin, Culberson County, Texas: M.S. Thesis, Stephen F. Austin State University, Nacogdoches, 234 p.

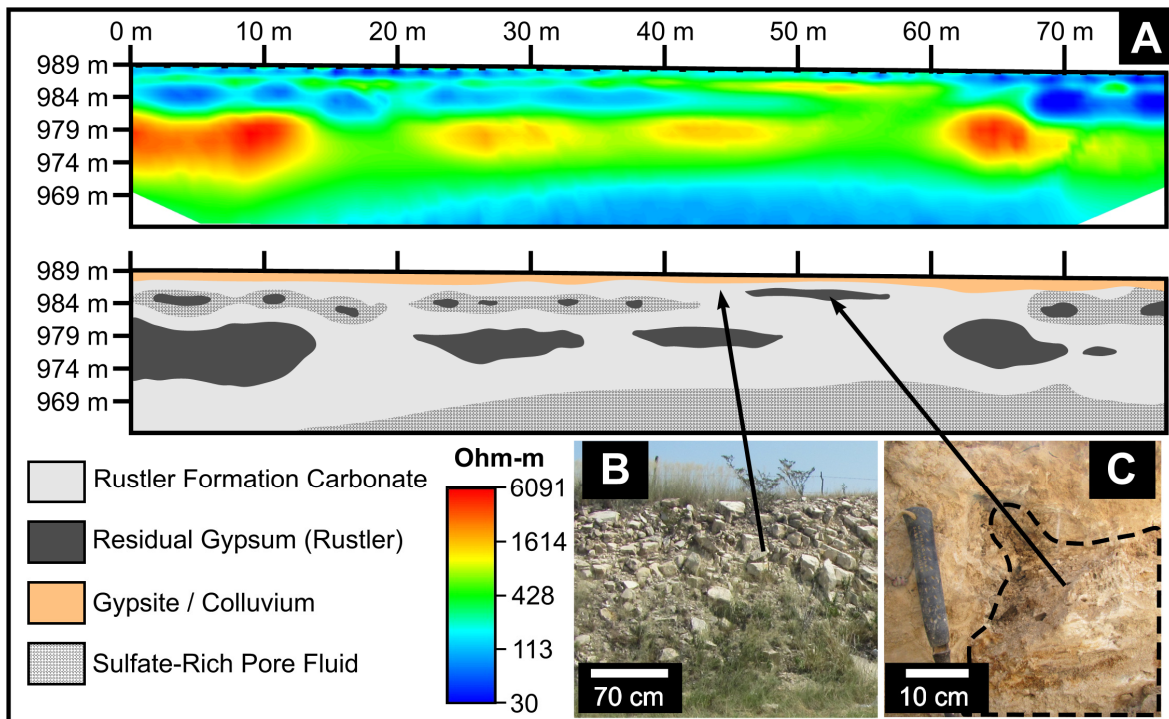


Figure 5. Intrastratal collapse geohazard (example 4): (A) DC electrical resistivity profile (RMS error = 2.97%) and associated interpretation of near-surface Rustler strata; incomplete, intrastratal dissolution of gypsum facies is being solutionally removed through increased meteoric recharge in infrastructure cut sections; (B) typical, highly fractured and partially collapsed Rustler carbonate in roadcut resulting from intrastratal dissolution of evaporite facies; and (C) leached gypsum (outlined by dashed line) in shallow subcrop.